

Detailed Experimental Study of Silicon Integrated Waveguide Modulator Achievable Through a Hybrid Structure of JFET and *p-i-n* Diode

Ricky W. Chuang^{1,2,*}, Mao-Teng Hsu¹, Zhen-Liang Liao¹, and Chih-Chieh Cheng¹

¹Institute of Microelectronics, Department of Electrical Engineering, and Advanced Optoelectronic Technology Center (AOTC), National Cheng Kung University, Tainan City 70101, Taiwan, R.O.C.

²National Nano Device Laboratories, Tainan County 74147, Taiwan, R.O.C.

*Corresponding Author's Phone and Email: +886-6-2757575 ext. 62397 and rwchuang@mail.ncku.edu.tw

INTRODUCTION

In recent years, a gradual maturity in silicon photonics technology has finally offered a golden opportunity for low-cost optoelectronic solutions in numerous applications including traditional telecommunications and newly emerged chip-to-chip interconnects [1-2]. In particular, implementing optical waveguides in place of electrical wires traditionally made out of aluminum or copper for signal transmission leads to astonishingly larger information-carrying capacity because of wider bandwidth and high data transfer rate. In order to successfully deliver all-photonics solutions for foregoing applications, the needs for signal routing and switching ultimately depend on the functionalities offered by optical modulators.

Since the modulation of silicon is predominantly and most efficiently achieved by carrier injection or plasma dispersion [3], both *p-i-n* diode [4-5] and transistor [6-9], therefore, are two of most frequently adopted device structures for the designs of silicon modulators. Previously, we had managed to fabricate junction field-effect transistor (JFET)-based silicon waveguide modulators with modulation depth close to 100% at $V_{DS} = \pm 5V$ when 5 mA gate current was administered [9]. Due to the subtleties of the processes involved in the fabrication and characterization of modulators, we believe that there are still quite a few delicate issues deserved to be fully explored in greater details. For example, our previous results [9] had shown that the modulation depth of devices measured was relatively insensitive to the magnitude of gate current and modulation length, except for devices with short modulation lengths. The foregoing results are in fact counterintuitive, and therefore further analyses are definitely required in order to decipher the inherent paradox.

This work provides a detailed study on a single mode silicon optical waveguide modulator incorporating a hybrid structure of junction field-effect transistor (JFET) and *p-i-n* diode for signal modulation. Again, the single mode waveguide condition is to be achieved based on a rib waveguide structure with a large cross-section [10-11], while the relevant waveguide dimensions such as rib width/height and the neighboring slab waveguide thickness are to be decided based on the simulation results of Beam Propagation Method (BPM). In this study, our emphases will be placed on investigating issues related to the dynamic and electro-optical performance of silicon modulators.

EXPERIMENTS

The relevant process involved in fabricating the aforementioned silicon light intensity modulators has already been reported elsewhere [9]. Again, the modulators consisting of different waveguide widths (5 to 15 μm) and various modulation lengths (100 to 9000 μm) were subsequently realized for further device characterization. The resultant device is schematically shown in Fig. 1 for detail. To ensure a single mode operation, the height of Si core is $\sim 7.5 \mu\text{m}$ and the height of slab region on each side of the rib waveguide was kept around $6.5 \mu\text{m}$. As being reported previously, the spin-on dopant (SOD) method was adopted to form the heavily doped p^+ and n^+ regions and the corresponding *p*- and *n*-type dopant profiles were determined using the spreading resistance probe (SRP) technique. The average dopant concentrations of both the

heavily doped p^+ and n^+ regions were in the neighborhood of 2 to $4 \times 10^{20} \text{ cm}^{-3}$. In addition, the average diffusion depths of p^+ and n^+ regions were between ~ 1.3 and $1.6 \mu\text{m}$.

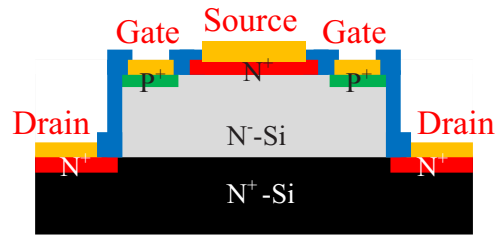


FIG. 1. A schematic drawing of silicon optical modulator incorporating a hybrid structure of JFET and *p-i-n* diode.

RESULTS AND DISCUSSION

The operation of the modulator was demonstrated by employing 1.5 μm continuous-wave (cw) InGaAsP-based laser diode as a light source, a germanium (Ge) photodiode as a output power detector, and a charge-coupled device (CCD) camera as a tool for observing the near-field output beam profile. The laser beam was coupled into the waveguide modulator in normal direction, and both input and output ends of the modulator were polished in order to increase the coupling efficiency. The CCD camera turned out to be a convenient apparatus for observing the motion of injected carrier plasma while the modulator was under the proper biasing condition. As shown in Fig. 2, when the drain-source voltage (V_{DS}) was increases from 0 to 11 V, a gradual disappearance of light spot in the central active region was clearly observed, indicating the input light was

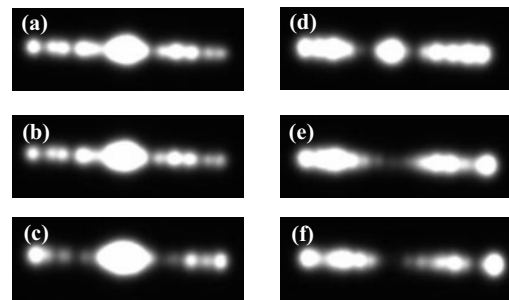


FIG. 2. A gradual disappearance of light spot from the central active region as observed when the modulator was biased with drain-source voltage (V_{DS}) of (a) 0 V, (b) 3 V, (c) 6 V, (d) 9 V, (e) 10 V, and finally (f) 11 V.

virtually absorbed by the injected carriers as result of carrier absorption. In this very example, $V_{DS} = 0 \text{ V}$ corresponded to the OFF state with the maximum output power P_{max} , while $V_{DS} = 11 \text{ V}$ corresponded to the ON state with the minimum output power P_{min} detected. In order to elucidate the effects of modulator's geometrical dimensions on its modulation capability, a series of modulation measurements was carried out. As depicted in Fig. 3, while setting the rib waveguide width constant (here, $W = 13 \mu\text{m}$), as the modulation length was lengthened, the corresponding device modulation efficiency was noticeably improved; that is, the required V_{DS} magnitude for achieving a nearly 100% modulation depth became smaller as needed. Part of reasons for this

observation could be due to a relatively larger number of injected carriers supplied by a modulator with a longer modulation length, enabling them to participate in the carrier absorption process. On the other hand, as shown in

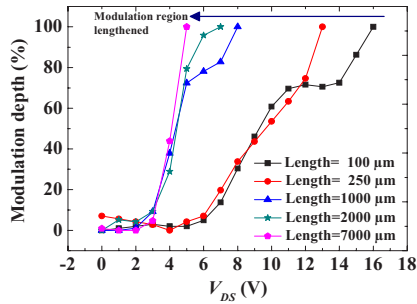


FIG. 3. The modulation depth versus V_{DS} measurement result for modulators of different modulation lengths, while their rib waveguide width was set at $W = 13 \mu\text{m}$.

Fig. 4, as the rib waveguide width was widened while keeping the modulation length constant (here, $L = 2000 \mu\text{m}$), similar enhancement in the modulation capability of the modulators was also observed.

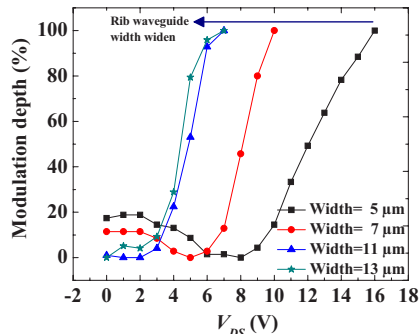


FIG. 4. The modulation depth versus V_{DS} measurement result for modulators of different rib waveguide widths, while their modulation length was set at $L = 2000 \mu\text{m}$.

In order to study the frequency response of these devices, that is, the frequency dependency of the corresponding modulation depth, the drain-source AC voltage signal (v_{DS}) and gate-source AC voltage signal (v_{GS}) of different frequencies were applied across the respective terminals. When 500 Hz v_{DS} signal was applied, the measured rise time (10% to 90% of maximum optical signal) and fall time (90% to 10% of maximum optical signal) were respectively determined to be 430 and 340 μsec . The corresponding oscilloscope waveforms are shown in Fig. 5. On the other hand, when v_{GS} of 500 Hz was applied, the respective rise and fall times were measured to be 440 and

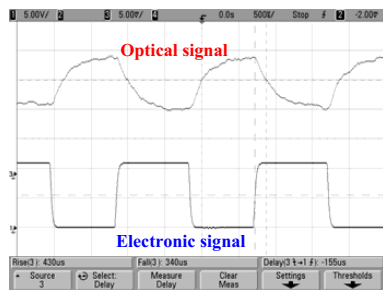


FIG. 5. The oscilloscope waveforms showing the 500 Hz electronic driving v_{DS} and the corresponding modulated light signals for the silicon modulator. The scales of the optical and electronic signals are 5 mV/div and 5 V/div, respectively.

520 μsec . Part of reason for obtaining a relative quicker response from a modulator biased by v_{DS} was because the highly mobile electron was only type of carrier participated in the modulation process, while for the other case involving the bias of v_{GS} , the slow-moving hole was also

engaged along with electron in the similar modulation event.

Finally, the frequency dependency of modulation depth for a modulator biased by v_{DS} is shown in Fig. 6 for reference. As Fig. 6 clearly demonstrates, the modulation efficiency of the foregoing device is deteriorated as the applied frequency of the electronic signal becomes higher. The result is understandable since it would become increasingly difficult for carriers to follow the applied signal as its frequency became higher. Similar results were also obtained for modulators biased by v_{GS} .

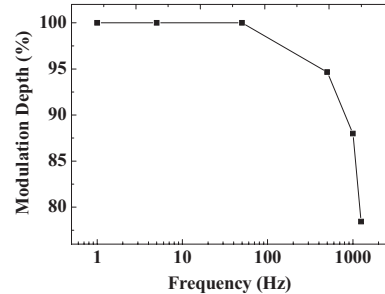


FIG. 6. The frequency dependency of modulation depth for a silicon modulator biased by v_{DS} .

CONCLUSIONS

In summary, we have successfully demonstrated a working silicon three-terminal transistor-based waveguide modulator; most of all, the dependencies of the modulation depth on the device dimensions and applied biasing signals of different frequencies were studied in full details. The corresponding measurement results will be reported during the upcoming SSDM 2008 conference.

REFERENCES

- [1] G.T. Reed, "The optical age of silicon," *Nature*, vol. 427, pp. 595-596, 2004.
- [2] International Technology Roadmap for Semiconductors (ITRS), 2006 Edition, Interconnect topic.
- [3] R. A. Soref and B. R. Bennett, "Electrooptical effects in silicon," *IEEE J. Quantum Electron.*, vol. QE-23, no. 1, January 1987.
- [4] C. K. Tang and G. T. Reed, "Highly efficient optical phase modulator in SOI waveguides," *Electron. Lett.*, vol. 31, no. 6, pp. 451-452, 1995.
- [5] R. W. Chuang and M.-T. Hsu, "Silicon optical modulators in silicon-on-insulator substrate based on the $p-i-n$ waveguide structure," *Jpn J. Appl. Phys.*, vol. 46, no. 4B, pp. 2445-2449, 2007.
- [6] R. D. Lareau, L. Friedman, and R. A. Soref, "Waveguided electro-optical intensity modulation in a Si/Ge_xSi_{1-x}/Si heterojunction bipolar transistor," *Electron. Lett.*, vol. 26, pp. 1653-1655, 1990.
- [7] A. Sciuto, S. Libertino, A. Alessandria, S. Coffa, and integrated Si-based light modulator," *J. Lightwave Technol.*, vol. 21, no. 1, pp. 228-235, 2003.
- [8] A. Sciuto, S. Libertino, S. Coffa, and G. Coppola, "Miniaturizable Si-based electro-optical modulator working at 1.5 μm ," *Appl. Phys. Lett.*, vol. 86, pp. 201115/1-201115/3, 2005.
- [9] Ricky W. Chuang, Zhen-Liang Liao, Mao-Teng Hsu, Jia-Ching Liao, and Chih-Chieh Cheng, "Silicon electro-optic modulator fabricated on silicon substrate utilizing the three-terminal transistor waveguide structure," *Jpn. J. Appl. Phys.*, vol. 47, no. 4, pp. 2945-2949, 2008.
- [10] R. A. Soref, J. Schmidtchen, K. Petermann, "Large Single-Mode Rib Waveguides in GeSi-Si and Si-on-SiO₂," *J. Quantum Electronics*, vol. 27, no. 8, pp. 1971-1974, 1991.
- [11] S. Pogossian, L. Vescan, and A. Vonsovici, "The Single Mode Condition for Semiconductor Rib Waveguides with Large Cross Section," *J. Lightwave Technol.*, vol. 16, no. 10, pp. 1851-1853, 1998.